CrystEngComm

Accepted Manuscript

ROYAL SOCIETY OF CHEMISTRY

www.rsc.org/crystengcomm

Cite this: DOI: 10.1039/c0xx00000x

www.rsc.org/xxxxxx

ARTICLE TYPE

Controlled synthesis of Co_3O_4 single-crystalline nanofilm enclosed by (111) facets and exceptional activity in the catalytic of ammonium perchlorate

Jun Wang, [a,b] Zhiqiang Qiao[a],Long Zhang[b],Jinpeng Shen[b],Rui Li[b], Guangcheng Yang *[a, b] and Fude Nie[a]

Received (in XXX, XXX) XthXXXXXXXXX 20XX, Accepted Xth XXXXXXXXX 20XX
DOI: 10.1039/b000000x

Single-crystalline, thermally stable, Co_3O_4 (111) nanofilm have been successfully synthesized without any surfactant. The catalytic activity of Co_3O_4 nanofilm is investigated via the thermal decomposition of ammonium perchlorate (AP). The AP exhibited unprecedentedly low decomposition temperatures and fast reaction rates in the catalyzed formations make Co_3O_4 (111) nanofilm as effectively catalyst.

The development of novel nanostructured transition metal oxides with controlled morphologies has stimulated considerable research interest for their unique properties and potential applications in materials science, physics and chemistry[1-4]. Co_3O_4, as an important transition metal oxide, is widely studied for its application in heterogeneous catalysts[5], field-emission materials[6], electrochemical devices[7,8], gas sensors[9], magnetic materials[10], anode materials in Li ion rechargeable batteries (LIBs)[11] and so on[12-13]. In recent years, Co_3O_4 nanocrystals with diverse structures have been successfully synthesized by different methods[14-25].

Since the discovery of graphene in the year of 2004, great efforts have been made to synthesize ultrathin layered structural materials such as nanosheets or nanofilm and explored their distinctive properties[26,27]. More recently, transition metal oxides (TMOs) have attracted tremendous attention due to their unique dimension-dependent properties. By assembling nanocrystals into the two-dimensional (2D) layered materials, novel electronic properties and high specific surface areas accompanying the enhancement of the host capabilities have been obtained and widely used in applications ranging from electronics to energy storage[28,29]. Many efforts have been made to design and develop the 2D materials[30,31]. Moreover, different crystal facets have different surface atom densities, electronic structure, bonding energy and possible chemical reactivity. Therefore, it is important to prepare transition metal oxide nanocrystals with exposed high-energy surfaces due to these facets can endow nanocrystals with a high activity, thus facilitating their potential applications such as highly efficient catalysts[32,33]. Typically, transition-metal oxides enclosed (111) facets with rock salt structure have high surface reactivity, consisting of alternating polar monolayer of anions and cations. Li et al investigated the effect of crystal plane on electrochemical performance, which revealed that Co_3O_4 octahedral enclosed by eight (111) facets show significantly enhanced electrochemical performance compared to (100) and (001) facets[34]. Hu et al synthesis single-crystalline Co_3O_4 (111) holey nanosheets which show highly active heterogeneous catalysts for methanol decomposition[35]. However, nanofilm with defined crystal planes on surface has not been widely studied due to less existing knowledge for their preparation. On the other hand, because of the existence of van der Waals interaction in layered structure, it is prone to heavy aggregation after drying and even be subsequently formed to bulk materials[36,37]. This probably results in the loss of the unusual properties of layered materials and shows no different properties compared with bulk materials. Organic surfactants are used to control the growth tendency to prevent these undesired processes[38, 39]. Unfortunately, the using of organic surfactants increases the cost and not environment friendly. Therefore, the controlling of materials agglomeration effectively with well-defined morphologies in a convenient way which is also environmentally friendly still remains a great challenge.

Ammonium perchlorate (AP) is the most widely used energetic material. It is an important oxidizer used in solid rocket propellants and thermal decomposition characteristics of AP directly influence the combustion behavior of the propellant. Numerous transition metal oxides are being evaluated for the thermal decomposition of AP[40-42]. As an important transition metal oxide, Co_3O_4 has been widely applied in catalytic decomposition of AP[43-47]. Lv synthesized Co_3O_4 nanoparticles enclosed by (111) facets and could greatly enhance the decomposition of AP[48]. However, few reports are found in literatures about the influence of catalytic activity of Co_3O_4 nanofilm enclosed by (111) facets on the decomposition of AP.

In the communication, the precursor of Co_3O_4 nanofilm was synthesized by microwave-assisted method and subsequent liquid nitrogen cooling using sodium hydroxide and cobalt nitrate solution. Single-crystalline Co_3O_4 (111) nanofilm was prepared after annealing at 320 °C for 2 h in air. The catalytic activity was also characterized by the thermal decomposition of AP. The present catalytic activity of single-crystalline Co_3O_4 (111) nanofilm show unprecedentedly low decomposition temperatures and fast reaction rates on the decomposition of AP.

The morphologies of the as-prepared samples were studied by field-emission scanning electron microscopy (FE-SEM). Fig.1(a) shows a low-magnification SEM image of Co_3O_4 membrane. The

cross-sectional SEM image shown in Fig. 1(b) reveals thatthe samples have highly layered morphology consisting of well arranged 2D nanofilm. Fig.1(c) shows that the as-prepared samples are mainly composed of nanofilm with curly shape and long-range structure with length almost dozens micrometer. Fig.1(d) shows a high magnification SEM image of the ultrathin Co_3O_4 nanofilm, which reveals that the large 2D film are rather thin with a typical thickness of about 30-40 nm (Figure1S). In addition, the high-magnification SEM image of the Co_3O_4 nanofilm clearly shows that the surface of the sheets is not totally smooth, but rough with lots of convex and concave topography. In order to optimize the morphology of the as-synthesized Co_3O_4 nanofilm and reveal the formation mechanism, the effect on the morphology of liquid nitrogen cooling is investigated (Figure 2S). Based on the experimental results, a possible formation mechanism concern the growth of Co_3O_4 nanofilm: Firstly, Co^{2+} ions and OH^{-1} reacted in solution in micro-wave oven to produce precursor crystal nucleus. Secondly, a large number of small nucleus undergo a self-assembly process and arrange to oriented nanosheets. The nanosheets further aggregate to form nanofilm with high surface area under liquid nitrogen cooling. The morphology of precursor show nano-particles without liquid nitrogen cooling (Figure 2S(a)). The specific surface area of the precursor is only 8.79 $m^2 \cdot g^{-1}$. However, the precursor shows large-area layered structure with a high surface area of 22.69 $m^2 \cdot g^{-1}$ with liquid nitrogen cooling after reaction. It should be attributed to liquid nitrogen cooling process result in a large number of crystal nucleus undergo a self-assembly process and arrange in oriented nanofilm. The low temperature also prevented nanofilm from aggregating to bulk material. The results reveal that liquid nitrogen cooling plays a significant role in the formation of large-scale nanofilm with high surface area.

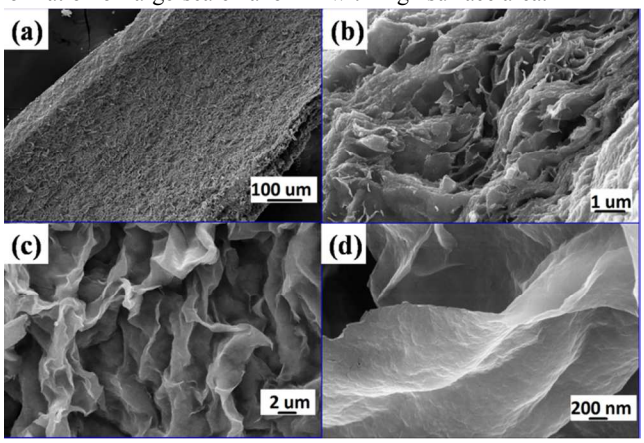

Fig.1 FE-SEM images of Co_3O_4(a):low-magnification SEM image, (b) FE-SEM image of a cross section region from (a), (c) and (d) high-magnification SEM images.

The powder X-ray diffraction (XRD) analysis of the as-prepared Co_3O_4 nanofilm after annealing at 320°C for 2 h in air is shown in Fig. 2(a). From the narrow peaks, it is clearly seen that the sample displays good crystalline features and well-defined diffraction peaks. The XRD pattern of the obtained products consists of eight diffraction peaks at 2θ values of 31.3°, 36.8°, 38.5°，44.7°, 55.7°, 59.4° and 65.2°, which are attributed to the (111), (220), (311), (222), (400), (422), (511) and (440) planes of the Co_3O_4 phase (JCPDS card No. 42-1467), respectively. This is also supported by the color change of the samples from the original blue to black. The XRD pattern and DSC-TG results reveal that the precursor is cobalt hydroxide (Figure 3S). Typically, crystallization of amorphous materials via heat treatment leads to undesired morphology. More interestingly, the nanofilm morphology of Co_3O_4 maintained after calcination. The surface area is 21.87 $m^2 \cdot g^{-1}$ after heat treatment at 320 °C, which is close to the precursor (22.69 $m^2 \cdot g^{-1}$). Furthermore, the intensity of the diffraction peaks increase along with increasing annealing temperature. The sample annealing at high temperature (420 °C) exhibits diffraction peaks higher than those of the other two samples annealing at low temperature, indicating its better crystalline features under high temperature (Figure.4S).

The more detailed composition of the products is further characterized by X-ray photoelectron spectroscopy (XPS), FTIR and Raman spectrum. The Co2p XPS spectrum (Fig.3(b)) shows two major peaks with binding energies at 770.6 and 794.7 eV, corresponding to $Co2p_{3/2}$ and $Co2p_{1/2}$, respectively. And the spin-energy separation is 14.9 eV, which is the characteristic of Co_3O_4 phase[17,18]. This result is consistent with the XRD data clearly. Two very strong peaks centered at 576 cm^{-1} and 672 cm^{-1} are noticed in FTIR spectrum, which is characteristic peaks of spinel Co_3O_4 (Figure.5s(a)). The Raman spectrum of the product measured at room temperature (Figure.5s(b)) displays four bands located at 475, 526, 621, and 693 cm^{-1}, corresponding to the Eg, F2g, F2g, and A1g modes of the spinel Co_3O_4 phase, respectively.

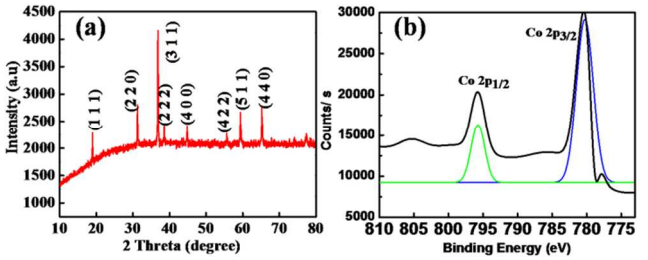

Fig.2(a) XRD pattern and (b) Co 2pXPS spectrum of Co_3O_4 nanofilm after annealing at 320°C for 2 h in air.

To further insight into the nature of the Co_3O_4 nanofilm, the morphologies and nano-crystalline properties were characterized by Transmission electron microscopy (TEM) and Selected-area electron diffraction (SAED). A typical TEM image (Fig. 3(a)) indicates that one of small film has an edge length of 6-8 um situated on the top of the copper grid. Moreover, from the TEM image, the Co_3O_4 nanofilm can be spread out on substrate, which is compatible with microsystem processing technique and have potential applications as micro-scale devices. The size is smaller than those shown in FESEM images, which may be resulted from its ruptured during ultrasonic treatment for TEM analysis. From the HRTEM of Fig.3(b), the sample was annealed at 320 °C for 2h in air, the interlayer spacing is about 0.46 nm, which corresponds to the interlayer distance of the (111) crystal plane of cubic Co_3O_4. We determine that the entire sheet is a single crystal with its surface perpendicular to (111) direction. The SAED analysis (the inset of (b)) indicates that the Co_3O_4 is quasi-single-crystalline in nature. The smaller spots are super-reflections which appear as a result of the ordered *Fd3m* structure of Co_3O_4. The SAED pattern displays a typical diffraction pattern of spinel Co_3O_4 consist further including the lattice plane of (111), (220), (311), (400), (422), (511) and (440) reflections. Therefore, single-

crystalline Co_3O_4 (111) nanofilm was obtained by annealing at 320 °C for 2h in air.

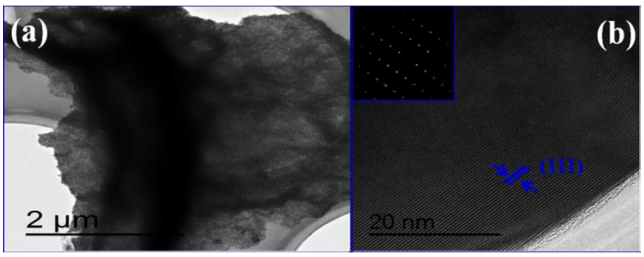

Fig.3 TEM and HRTEM images of the Co_3O_4 nanofilm. The inset of (b) shows SAED pattern of the Co_3O_4 nanofilm showing quasi-single-crystalline in nature.

Herein, the catalytic property of Co_3O_4 nanofilm was investigated by Differential Scanning Calorimetry (DSC), which was carried out under a Ar atmosphere (at a flow rate of 20 ml/min) with a heating rate of 5 °C/min. Co_3O_4 nanofilm and AP were mixed by ultrasonic vibration and then dried in air at 60 °C for 4 h. Fig.4 shows the DSC curves of pure AP and mixtures of AP and Co_3O_4 nanofilm. One endothermic peak at 242 °C is observed in Fig. 4, which attributed to the phase transition from an orthorhombic form to a cubic[45-46]. The exothermic peak appeared at 457 °C is corresponding to the decomposition of AP. It is shown that when different amount of Co_3O_4 nanofilm products were added to AP, all the samples have similar position of endothermic peak (242 °C), which reveal that the Co_3O_4 nanofilm products do not influence the crystallographic phase transition temperature of AP. However, as shown in the DSC curves, the introduction of Co_3O_4 catalysts has markedly decreased the temperature of the decomposition. Moreover, the decomposition temperature is varied from the amount of Co_3O_4 catalysts. The exothermic peak of 1%, 2% and 3% w/w Co_3O_4 nanofilm in mixture (Co_3O_4+ AP) is located at 303, 296, 271°C, respectively. Compared with pure AP, the exothermic peak of the mixture is decreased by about 124, 129, 155 °C, respectively. Compared with literatures[44-47], with introduction of 3wt% of our single-crystalline Co_3O_4 nanofilm with (111) facets into the AP, the AP exhibit much low exothermic peak. At the same time, the DSC curve of particle Co_3O_4 which has the similar special surface (28.93 m^2 g^{-1}) also been characterized by prepared the different Co_3O_4 catalytic particles. As Figure 6S shown that a higher peak temperature (316°C) than the same 3% w/w was obtained which exhibits that CO_3O_4 nanofilm with (111) facets has significant catalytic activity compared with particles. According to the former reports[35,36,48], the (111) plane has more Co^{2+} which is beneficial to catalyze decomposition of AP than other plane. Moreover, narrow temperature distribution (257-275°C) between the initial temperature and the final temperature show a fast rate of reaction of AP. From the above experimental results, it is found that Co_3O_4 nanofilm with (111) facets has significant catalytic activity, which is beneficial for the thermal decomposition of AP.

Kinetic parameters of AP decomposition with Co_3O_4 nanofilm additives were calculated from the exothermic peak temperature dependence as a function of heating rate via the Kissinger method (Table1s). The results reveal that AP with introduction of 3wt% Co_3O_4 nanofilm show remarkably increased rate of reaction and decreased activation energy.

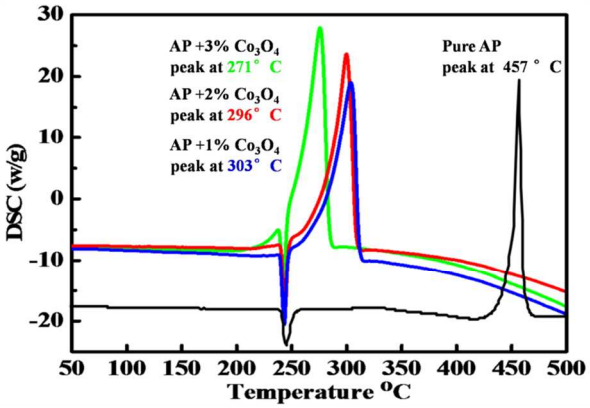

Fig. 4 DSC curves of pure AP, AP+1% w/w Co_3O_4 nanofilm, AP+2% w/w Co_3O_4 nanofilm, AP+3% w/w Co_3O_4 nanofilm

Conclusions

In summary, we have developed a simple and efficient method to synthesize single crystalline Co_3O_4nanofilmwith high exposed (111) facets. The liquid nitrogen cooling treatment during reaction plays a crucial role in the formation of Co_3O_4nanofilm with high surface area. The results suggested a high catalytic activity for Co_3O_4nanofilm to decompose AP and AP exhibited unprecedentedly low decomposition temperatures and fast reaction rates. Co_3O_4 nanofilm has potential applications as micro-scale devices. This work provides us a simple and convenient method for preparing controlled nanostructured transition metal oxide with defined crystal planesto meet the demand for diversity.

Acknowledgements

This work was supported by the National Natural Science Foundation of China (No. 11272292, 11372288, 11172275 and 11172276),National High Technology Research and Developmen t Program of China (863 Program) (No. 2013AA050905), Science Foundation for Young Scientist of Sichuan Province (2012JQ0038), and Young Talent Foundation of Institute of Chemical Materials (QNRC 201201 and QNRC 2013-10).

Notes and references

[a] *Institute of Chemical Materials, China Academy of Engineering Physics,No. 64, Mianshan Road, Mianyang City, China. Fax: (86) 8162544426; Tel: (86) 8162482005; E-mail: ygcheng@hotmail.com*

[b] *Sichuan New Material Research Center, No.20, yuan yi street, Mianyang, China. Tel: (86) 8162544436; E-mail: wjnjun@163.com*

† Electronic Supplementary Information (ESI) available: [FE-SEM images of the Co_3O_4 nanofilm, FTIR curves and Raman spectrum of products]. See DOI: 10.1039/b000000x/

1 S. Mann and G. A. Ozin, Nature, 1996, 382, 313.
2 M. A. El-Sayed, Acc. Chem. Res., 2004, 37, 326.
3 Z. X. Xiao, C. Y. Han, W. K. Kwok, U. Welp, J. Wang and G. W. Crabtree, J. Am. Chem.Soc., 2004, 126, 2316.

4 S. Masaoka, D. Tanaka, H. Kitahaka,S. Araki, R. Matsuda, K.Yoshikawa, K. Hato, M. Takata and S. Kitagawa, J. Am. Chem. Soc., 2005, 127, 5662.

5 L. P.Zhou, J.Xu, H.Miao, F.Wang and X. Q. Li, Appl. Catal.A.2005,292,223-236.

6 T.Yu, Y. M.Zhu, X. J.Xu, Z. X.Shen, P.Chen, C. T.Lim, J. T. Thong and C. H.Sow, Adv. Mater. 2005,17,1595-1598.

7 W. Mei, J. Huang, L. Zhu, Z. Ye, Y. Maia and J. Tu, J. Mater. Chem., 2012,22, 9315-9321.

8 C. Yuan, L. Yang, L. Hou, L. Shen, X. Zhang and X. W. Lou, Energy Environ. Sci., 2012, 5, 7883-7889.

9 T. Akamatsu, T. Itoh, N. Izu, W. Shin, scensors, 2013, 13, 12467-12481.

10 C. Nethravathi, S. Sen, N. Ravishankar, M. Rajamathi, C. Pietzonka and B. Harbrecht, J. Phys. Chem.B. 2005,109,11468-114873.

11 W. Y. Li, L. N. Xu and J. Chen, Adv. Funct. Mater,2005,15,851-856.

12 E. Hosono, S. Fujihara, I. Honma and H. S.Zhou, J. Mater.Chem. 2005,15,1938-1943.

13 Y. G.Li, B.Tan and Y. Y.Wu,J. Am. Chem. Soc. 2006,128,14258-14261.

14 X. H. Xia, J. P. Tu, Y. J. Mai, X. L. Wang, C. D. Gu and X. B. Zhao,J. Mater. Chem., 2011, 21, 9319-9323.

15 S. N. Karthick, K. V. Hemalatha, C. Justin andM. Yi. J Nanopart Res 2013, 15,1474-1477.

16 D. S. Wang, T. Xie, Q. Peng, S. Y. Zhang, J. Chen and Y. D. Li,Chem.Eur. J., 2008, 14, 2507-2512.

17 S. K. Meher and G. R. Rao, J. Phys. Chem. C, 2011,115,15646-15650.

18 S.L.Xiong, C.Z.Yuan, M.F.Zhang, B.J.Xi and Y. T. Qian, Chem.Eur. J. 2009,15, 5320-5324.

19 Y.Q.Fan, H.Shao, J. Wang, L.Liu, J. Zhang and C. Cao, Chem.Commun.2011,3469-3471.

20 F. Zhan, B. Geng, Y. Guo, Chem. Eur. J. 2009, 15, 6169-6174.

21 X. Wang, X. L. Wu, Y. G. Guo, Y. Zhong, X. Cao, Y. Ma, J. Yao. Adv. Funct. Mater, 2010,1680-1686.

22 J. P. Tu, X. L. Wang, C. D. Gu and X. B. Zhao, Chem. Commun., 2011, 47, 5786-5788

23 U. Tong, J. Guan and Q. J. Zhang. Adv. Funct. Mater., 2013,23, 2405-2409.

24 Y. G. Li, B. Tan, and Y. Y. Wu, Nano Lett., 2008,8, 265-268.

25 G. L. Wang, D. X. Cao,C. L. Yin, Y.Y. Gao, J. Yin, and L. Cheng, Chem. Mater. 2009, 21, 5112-5118.

26 K. S.Novoselov, D.Jiang, F.Schedin,T. J.Booth, V. V.Khotkevich,S. V.Morozov, A. K.Geim, Proc. Natl. Acad. Sci. U.S.A. 2005, 102, 10451.

27 K. S. Novoselov,V. I. Fal'ko, L. Colombo, P. R.Gellert, M. G. Schwab and K. Kim, Nature, 2012, 490, 192-196.

28 R. Ma and T. Sasaki, Adv. Mater. 2010,22,5082-5085.

29 J. A. Rogers, M. G. Lagally, R. G. Nuzzo, Nature, 2011, 477, 45-49.

30 J. W.Seo, Y.W.Jun, S.W. Park, H.Nah,T.Moon, B.Park,J. G.Kim and Y. J.Kim, J. Angew. Chem.2007,119, 8984-8987.

31 Y.Tatsuto,M. Yumiko, Takako Tsuchino, T. Itoh and T. Hattori, Chem. Mater. 2005, 17, 206-211.

32 X. Xie, Y. Li, Z.-Q. Liu, M. Haruta and W. Shen, Nature, 2009, 758, 746-749.

33 N. Tian, Z. Y. Zhou, S. G. Sun, Y. Ding and Z. L. Wang, Science,2007, 316, 732-736.

34 X. L. Xiao, X. F. Liu, H. Zhao,D. F. Chen, F. Z Liu, J. Xiang,Z. B. Hu andY. D. Li, Adv. Mater,2012,24,5762-5766.

35 L. F. Chen, J. C. Hu, R. Richards, S. Prikhodko and S. Kodambaka, Nanoscale, 2010, 2, 1657-1660.

36 P. D.Antunez,J. J.Buckley andR. L.Brutchey, Nanoscale, 2011, 3,2399-2403.

37 V. Nicolosi, M. Chhowalla, M. G. Kanatzidis,M. S. Strano and J. N. Coleman, Science,2013,340,1226419-1226421.

38 T.He,D. R. Chen, X. L.Jiao, Y. L.Wang and Y. Z.Duan,Chem. Mater. 2005,17,4023-4027.

39 S. Z. Butler,S.M. Hollen, L. Cao, Y. Cui. ACS nano, 2013,7,2898-2926.

40 Z. X. Zhou, S. Q. Tian, D. W. Zenga, G. Tang and C. S. Xie, Journal of Alloys and Compounds, 2012,513,213-219.

41 R. A. Chandru, S. Patra, C. Oommen, N. Munichandraiah and B. N. Raghunandana ,J. Mater. Chem., 2012,22, 6536-6538.

42 M. Zou, X. Jiang, L. Lu, X. Wang. J. Hazard. Mater., 2012,225-226,124-130.

43 T. D. Hedman,D. A. Reese, K. Y. Cho, L. J. Groven, R. P. Lucht and S. F. Son,Combust. Flame., 2012,159,1748-1758.

44 L. N. Jin, Q. Liu, W. Y. Sun.CrystEngComm, 2012,14, 7721-7726.

45 J. Zhao, Z. S. Liu, Y. L. Qin and W. B. Hua, CrystEngComm, 2014,16, 2001-2008

46 C. Xu, X. Wang, J. W. Zhu, X. J Yang and L. L. Lu, J. Mater. Chem., 2008, 18, 5625-5629.

47 W. Q. Pang, X. B. Shi and Y. Li, Adv. Mater. Research,2012,284,560-561.

48 H. zhou, B. L. Lv and D. Wu, CrystEngComm, 2013,15,7443-7449.